Heliyon

Received:
5 December 2017
Revised:
9 April 2018
Accepted:
1 August 2018

Cite as:
Mohammad W. Marashdeh. Effect of the LEGe detector collimators on K-series peaks and Compton scattering in XRF analysis using gamma rays.
Heliyon 4 (2018) e00724.
doi: 10.1016/j.heliyon.2018.e00724

Effect of the LEGe detector collimators on K-series peaks and Compton scattering in XRF analysis using gamma rays

Mohammad W. Marashdeh*

Department of Physics, College of Sciences, Al Imam Mohammad Ibn Saud Islamic University (IMSIU), P.O. Box 90950, Riyadh 11623, Saudi Arabia

* Corresponding author.

E-mail addresses: mwmarashdeh@gmail.com, mwmarashdeh@imamu.edu.sa (M.W. Marashdeh).

Abstract

The effect of a low-energy germanium detector collimator with different diameters on the measurement of the X-ray fluorescence of palladium (Pd) was studied experimentally. Changes in the Pd K-series and Compton scattering peaks were measured and analysed with and without a detector collimator, where for the former, collimators with different diameters were used. The signal-to-noise ratio increased when a shielding collimator was used with a narrow detector collimator. The Compton dispersion and fraction dead time were reduced considerably using a detector collimator by increasing the distance from the source to the detector, and the collimator length-to-diameter ratio. The full width at half maximum (FWHM) of the Pd $K_{\alpha 1}$ and Pd $K_{\beta 1}$ peaks decreased almost linearly with the collimator length-to-diameter ratio. The FWHM illustrated that the spectral resolution was improved when a collimator with a smaller diameter but unchanged length was used. The uncertainties at the Pd $K_{\alpha 1}$, Pd $K_{\beta 1}$, and Compton dispersion peaks were approximately correlated linearly with the collimator length-to-diameter ratio.

Keywords: Atomic physics, Physics methods

https://doi.org/10.1016/j.heliyon.2018.e00724

1. Introduction

Absorption of the photoelectric layer, Compton scattering, and pair production are the three main interaction processes that play a significant role in the measurement of gamma radiation [1]. Among these processes, a multi-process high-order Compton scattering occurs because of the large amount of secondary radiation within the first encounter [2]. In the study of the interaction processes of gamma rays, these radiations are often encountered moving singly toward the detector as scattered radiation. Therefore, studies have suggested that multiple Compton scatterings may create difficulties in data interpretation, and therefore, radiations that present single scattering within the same energy range are preferred [2, 3].

The detector essentially needs to be collimated and protected to restrict the incident rays that strike the detector and reduce the detection of the background scattering radiation caused by cosmic rays or by the terrestrial radiation itself. This process increases the signal-to-noise ratio (SNR) [4, 5]. A shield is required to protect the user against the scattered radiation. Total collimation is an experimental system that is a compromise between linking the collimation of a detector with a low count and SNR deterioration because inadequate collimation of a detector will generate a wide Compton peak. Thus, a higher contribution of scattered radiation is obtained within the peaks of a fluorescent element [2, 6]. Beam collimation at a sample effectively affects the sensitivity of an X-ray fluorescence (XRF) system. In addition to maximizing the sensitivity of an XRF system, the collimation and source−sample distance should be selected such that the irradiated volume is consistent with the volume viewed by the detector. This requirement reduces unnecessary doses to the subject and decreases the energy range of the detected Compton scattered photons [7, 8]. When a narrow beam geometry is performed, the multiple scattered photons are prevented from reaching the detector and so are not measured. But as the collimator size (half acceptance angle) is increased, the probability of multiple scattered photons reaching the detector increases.

Studies on XRF systems have used collimators with various sizes, shapes, and materials based on the concentrated element. For example, a collimator in front of a detector was made from copper with an inlet diameter of 20 mm. Brass and copper have been used rather than lead to overcome the limitations of platinum detection [9]. Tungsten has also been used as a collimator material because of its maximum photon attenuation and higher potential for the separation of X-rays compared to lead [7]. Collimator detectors made of brass, with an inner diameter of 25 mm, and of lead, with an opening diameter of 15 mm, have also been applied [4, 7, 10, 11]. Both primary and secondary beams have been collimated using lead cylinders with an inner diameter of 25 mm for the scattered beams in the primary collimation, while brass tubes with a diameter of 25 mm and length of 250 mm have been

https://doi.org/10.1016/j.heliyon.2018.e00724

used for the scattered beams in the secondary collimation [9, 10, 11]. Lead cylinders with a length of 125 mm are made of stainless steel. Thus, studies have emphasized the use of lead cylinders and brass tubes with inner and outer diameters of 25 mm and 45 mm, respectively [12].

Several studies have shown the effects of a detector collimator and target thickness on the Compton scattering and K-series peaks through the use of different detectors, such as a sodium iodide (NaI), (Tl) and HPGe detectors [3, 6, 7]. However, the effect of a detector collimator on the Compton scattering using a low-energy germanium (LEGe) detector has not been investigated.

X-ray fluorescence is widely used to analyse the elemental and quantitative elements of different types of materials [13]. In addition, to study the attenuation of samples in the low-energy range, it is necessary to have a beam of radiation with discrete energies within this energy range. The XRF method can be used to determine the linear and mass attenuation coefficients of the samples [14]. Therefore, there are some factors that affect the detector collimators, and the detector-source distance is a critical factor that must be measured accurately and carefully.

In this study, the effects of lead collimator shielding and geometric parameters, such as the size of the collimator detector, on the K-series of Palladium (Pd) and the scatter backgrounds in an XRF setup were determined. The SNR, Compton scattering, fraction dead time, and peak resolution, represented by the full width at half maximum (FWHM), were investigated.

2. Materials and method

The detector and source were set up and arranged within approximately 180° with respect to the backscatter geometry (Fig. 1). The detector was a LEGe Canberra GL0210R with the following specifications: active area, 200 mm^2; active diameter

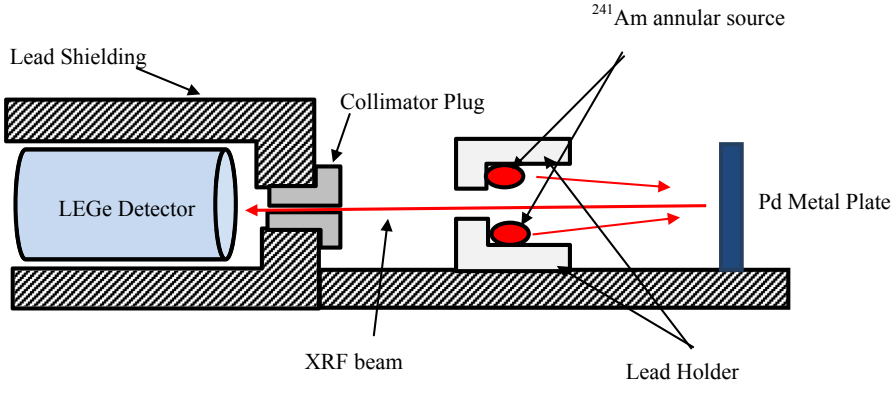

Fig. 1. Experimental setup of LEGe detector, ^{241}Am, the lead shielding and the collimation plug.

https://doi.org/10.1016/j.heliyon.2018.e00724

and thickness of 16 mm and 10 mm, respectively; and a beryllium window with a thickness of 0.15 mm, and 195 eV at 5.9 keV resolution. The detector was cooled by liquid nitrogen. The preamplifier used was a resistive feedback (RC) Canberra 2002CP. An annular americium-241 (^{241}Am) source was used as a gamma ray source, with radioactivity and energy of 100 mCi and 59.53 keV, respectively. This source was mounted on a lead holder, and it had three shutters consisting of a front lead shutter, facing the source, and two shutters (lead and aluminium) backing the source and facing the detector, respectively, to minimize the health hazards and background radiation [15]. In this study, all the shutters were open to obtain the XRF spectrum of the sample. The detector head was well-covered using lead shielding, with a sufficient thickness to protect it against scattered X-rays and to reduce the background counts that may originate from nearby X-ray equipment or radioisotopes. A lead collimation plug was also placed in front of the detector to enable the detector to view only the irradiation volume of the Pd metal plate. Lead-lined walls surrounded the setup to protect the user against scattered X-rays.

The photon spectra of the 241-Am gamma rays were recorded by increasing the distance between the source and the detector from 100 mm to 400 mm, while the distance between the source and the Pd metal plate was fixed at 30 mm. At the same time, a collimator with a diameter of 3 mm was used. LEGe detectors with and without collimator shielding were used in this step. The whole experiment was repeated by changing the size of the collimator and fixing the distance from the source to the detector and from the source to the Pd metal plate at 100 mm and 30 mm, respectively. These values were based on the nearest possible distance where the source and sample could be placed. Five collimators with diameters of 1, 2, 3, 4, and 5 mm and a fixed length of 50 mm were used to study the effect of the LEGe detector collimators on the Pd K-series and Compton scattering peaks. The Pd target was irradiated for 600 seconds, and the spectra were recorded and analysed using MAESTRO software. The temperature of the room was maintained at 22 °C by an air conditioner. The region of interest for the $K_{\alpha 1}$ peak energies was determined from the results of the spectrum of the Pd target. The channel number that corresponded to the peak energy was recorded. Next, the value of the net area was recorded as the XRF spectrum of the Pd metal plate target.

3. Results and discussion

A collimator plug helped to effectively reduce the Compton scatter. However, as the diameter of the detector collimator was reduced, the scatter background decreased significantly, as shown in Fig. 2. According to the figure, the number of Compton scattered events increased with an increase in the diameter of the detector collimator. For a collimator plug with a diameter of less than 2 mm, there were less variations in the number of counts of the Pd $K_{\alpha 1}$ and Pd $K_{\beta 1}$ peaks, but behind this collimator

https://doi.org/10.1016/j.heliyon.2018.e00724

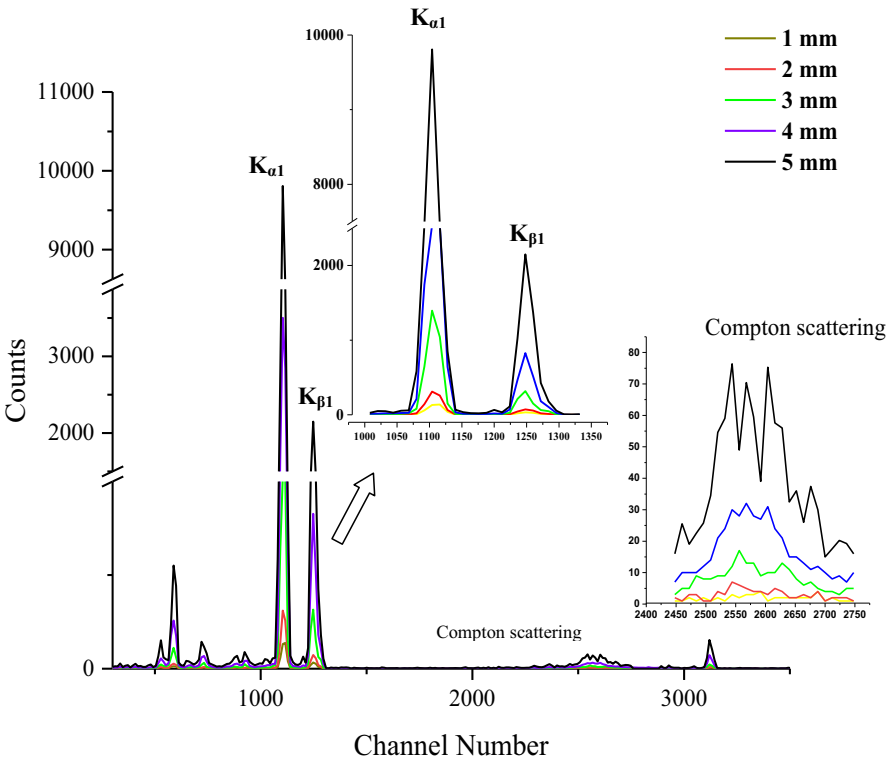

Fig. 2. $K_{\alpha 1}$, $K_{\beta 1}$, and Compton scattering peaks of the Pd metal plate with different collimator diameters (1, 2, 3, 4, and 5 mm).

diameter there was a marked increase in the counts of the Pd $K_{\alpha 1}$ and Pd $K_{\beta 1}$ peaks. The increase in the count rate of the Pd peaks was due to the fact that the height in the solid angle was subtended by the detector as the collimator opening increased. Thus, the XRF image of the Pd peak was obtained from an increased diameter of the collimator plug, which increased the acceptance angle of the front face of the LEGe detector.

3.1. Study of SNR

An important parameter for obtaining the greatest sensitivity measurement, namely, the signal-to-noise ratio (SNR), was applied to detect the minimum radiation detector sensitivity [7]. This concept is important for understanding the effect of the collimator plug of a detector on the quality of the radiation sensitivity control.

The SNR for the detection of minimum sensitivity is expressed as Eq. (1)

$$SNR = \frac{C_{Sample} - C_{bkg}}{C_{bkg}} \times 100\%, \tag{1}$$

where C_{Sample} is the rate of counting of the Pd sample, as well as background and C_{bkg} represents the rate of counting of the background without the Pd sample.

https://doi.org/10.1016/j.heliyon.2018.e00724

The SNR generally increased when a lead collimator plug was used. The ratios of the intensities of the Pd $K_{\alpha 1}$ and Pd $K_{\beta 1}$ peaks to the background with a collimator plug increased significantly compared to without the use of a collimator plug (Fig. 3). In addition, Fig. 4 shows that the collimator length and diameter had an impact on the SNRs of the Pd $K_{\alpha 1}$ and Pd $K_{\beta 1}$ peaks, where the SNR increased with an increase in the length-to-diameter (L/D) ratio of the collimator.

A collimator plug with a large diameter resulted in a low SNR, which indicated a higher count of the background scattering compared to the single count of the Pd peak. The presence of a higher background scattering compared to a single XRF peak (Pd peak) was observed in Fig. 4. The SNR could be increased by decreasing the background scattering of the photons. This phenomenon was possible with the use of a detector plug with a narrow diameter, which was in agreement with the findings of previous studies [6, 16].

3.2. Signal-to-Compton scattering ratio

The ratio of a peak to the Compton scattering is the relationship between the potential count number at the peak [17], N_x at a channel, X, and the average count number, $\overline{Nc}$ of the Compton allocation that lies below the rise and in the direction of the Compton edge (American National IEEE Standard), as shown in Fig. 5.

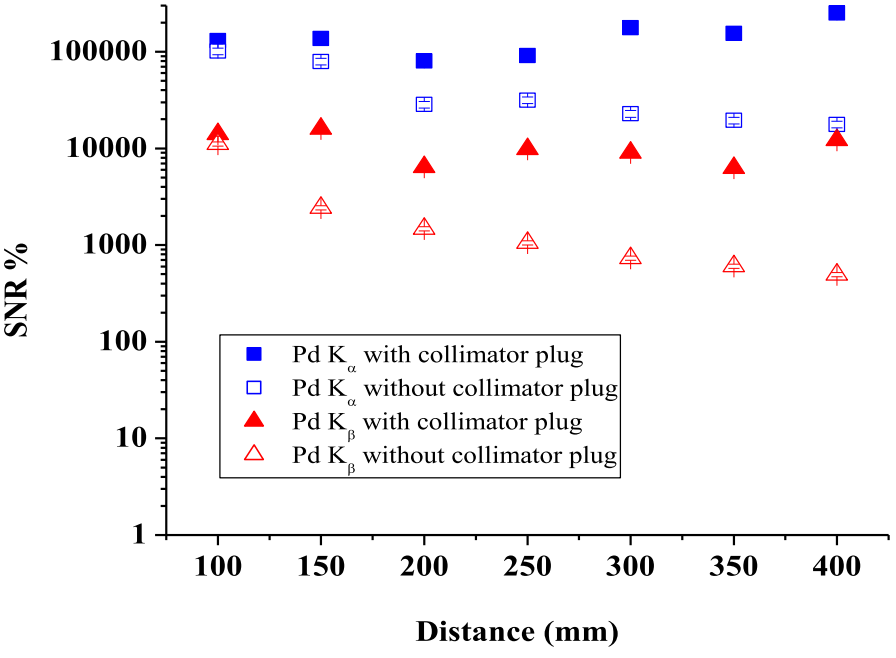

Fig. 3. Observed signal-to-noise ratios with variations in Pd $K_{\alpha 1}$ and $K_{\beta 1}$ with and without collimator plug versus distance from the source to the detector.

https://doi.org/10.1016/j.heliyon.2018.e00724

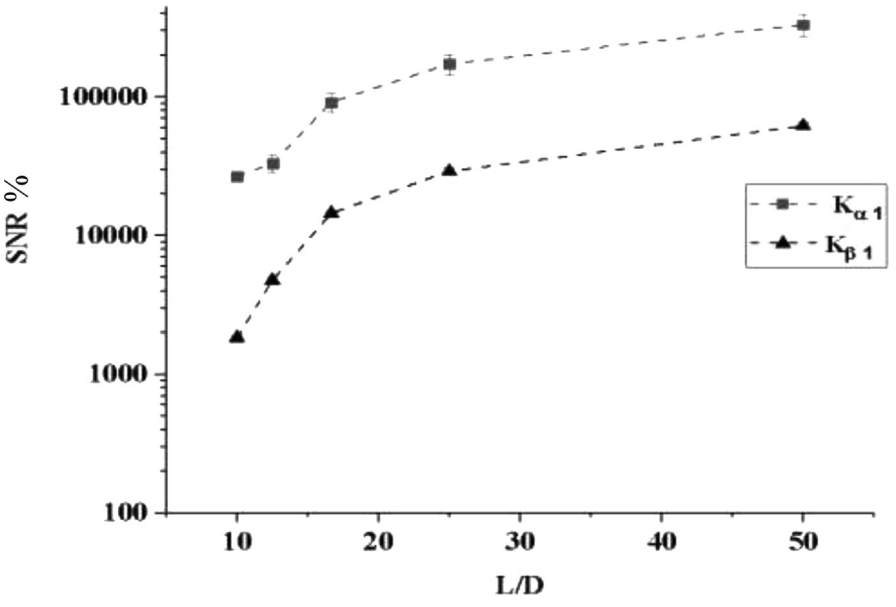

Fig. 4. Observed signal-to-noise ratio with variations in $K_{\alpha 1}$ and $K_{\beta 1}$ versus ratio of collimator length to diameter (L/D).

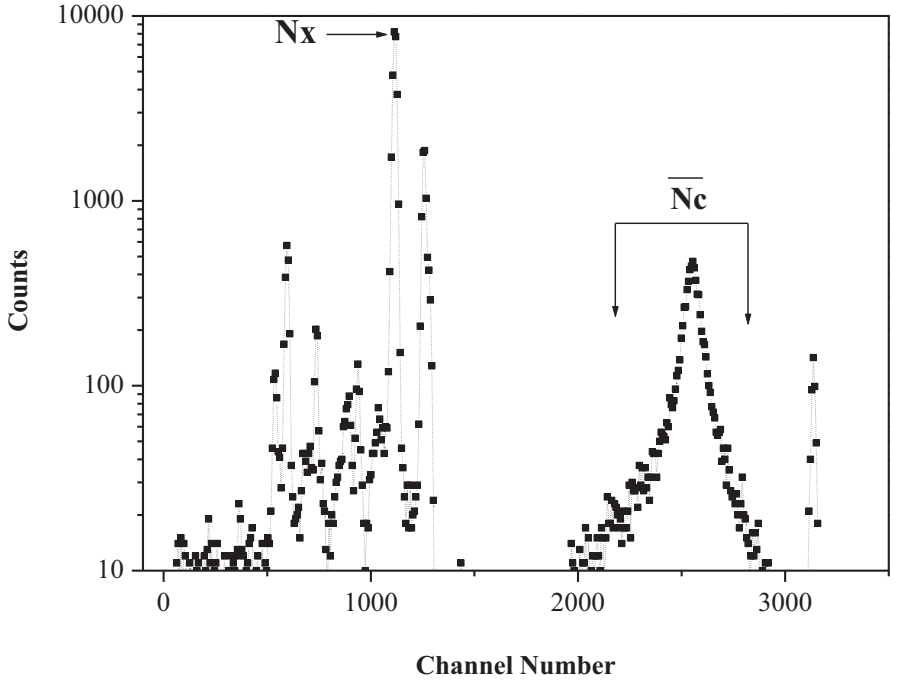

Fig. 5. Determination of Peak-to-Compton scattering ratio from Pd spectrum.

It is evident from Fig. 6 that the signal-to-Compton scattering ratio (SCR) increased with the use of a detector collimator plug compared to a detector without a collimator plug. On the contrary, the SCR with shielding was affected slightly by the distance between the source and the detector [17]. The ratio of the maximum count of the Pd

https://doi.org/10.1016/j.heliyon.2018.e00724

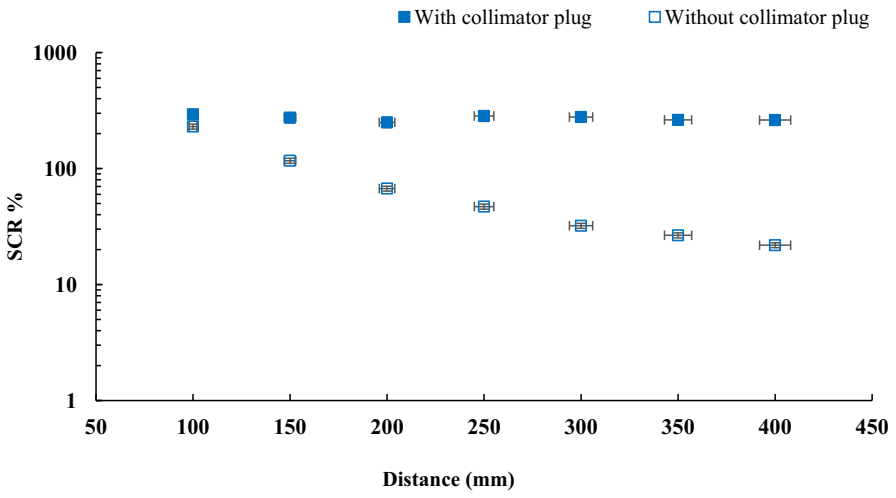

Fig. 6. Peak-to-Compton scattering ratio measured with Pd $K_{\alpha 1}$ as a function of distance from source to detector.

$K_{\alpha 1}$ at channel 1113 to the average region of Compton's distribution (at channel 2400−2700) increased linearly with an increase in the length-to-diameter ratio of the collimator. The pulses generated by the incident radiation were collected and binned into channels according to their amplitude. The intensity of Pd at the $K_{\alpha 1}$ peak decreased to such an extent as to eliminate the advantages of using the collimator. In addition, as shown in Fig. 7, when a collimator length (50 mm)-to-diameter (5 mm) ratio of 10 was used and the collimator was positioned in front of the detector, the Compton scattering at its peak intensity was higher than when a collimator with a diameter of 1 mm and a length of 50 mm (L/D = 50) was used. However, the SCR of the L/D = 10 remained smaller than the SCR of the

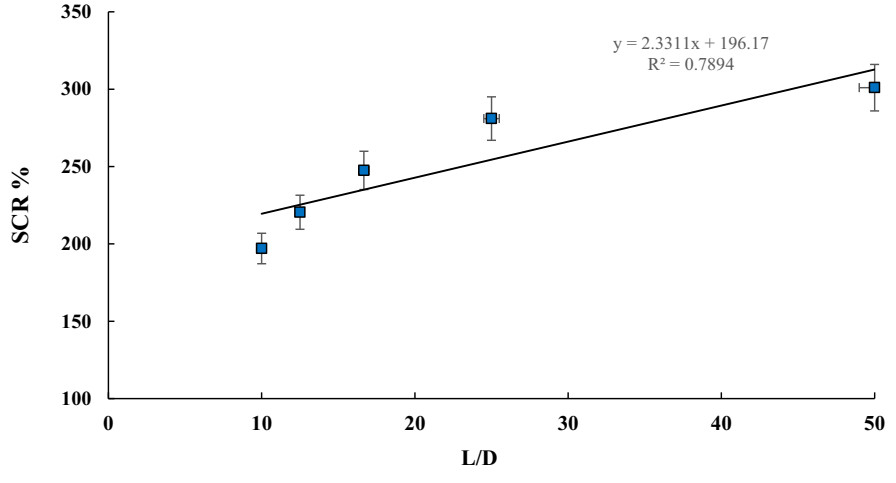

Fig. 7. Observed variation of peak-to-Compton scattering ratio for Pd $K_{\alpha 1}$ with the collimator length to diameter ratio (L/D).

https://doi.org/10.1016/j.heliyon.2018.e00724

L/D = 50, which led to the SCR being affected by the collimator diameter, in particular, and the shielding of the detector, in general. On the other hand, the SCR was higher for the collimator with a diameter of 1-mm than for the one with a diameter of 5 mm, where the fixed collimator length of 50 mm (L/D = 10) maximized the probability of the total absorption of the energy of the photons that were initially Compton-scattered within the detector. In fact, the collimator shielding of the detector with a larger SCR resulted larger SNRs and better counting statistics for the complex spectra.

3.3. Peak resolution represented as FWHM

The FWHM values at the Pd $K_{\alpha 1}$ and $K_{\beta 1}$ peaks with and without shielding were almost the same with slightly different source-to-detector distances (Fig. 8). This phenomenon was due to the fact that the photoelectric event exhibited the highest probability in the low-incident photon energy that was used (21.21 keV and 23.93 keV) for the Pd $K_{\alpha 1}$ and $K_{\beta 1}$ peaks, respectively. The L/D ratio of the collimator had an impact on the FWHM and peak resolution. The FWHM values at the Pd $K_{\alpha 1}$ and $K_{\beta 1}$ peaks depended linearly on the L/D ratio of the collimator (Fig. 9). A smaller collimator diameter with a collimator length of 50 mm reduced the divergence of the spectra, thereby increasing the peak resolution, as illustrated by the FWHM. This case could be seen clearly in the Pd $K_{\beta 1}$ peak because the FWHM of the Pd $K_{\alpha 1}$ peak was not significantly affected in view of the L/D ratio of the collimator.

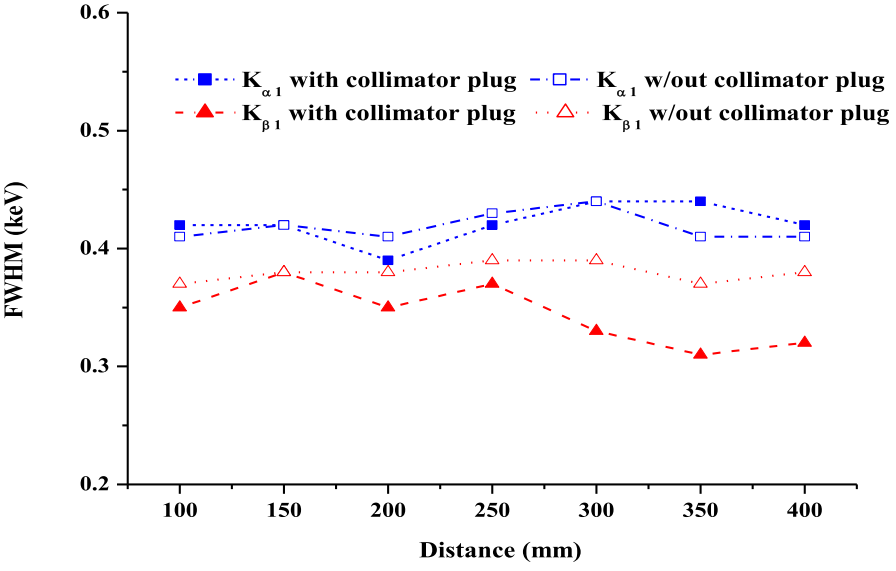

Fig. 8. Change in FWHM for Pd $K_{\alpha 1}$ and $K_{\beta 1}$ peaks with and without collimator plug versus distance from source to detector.

https://doi.org/10.1016/j.heliyon.2018.e00724

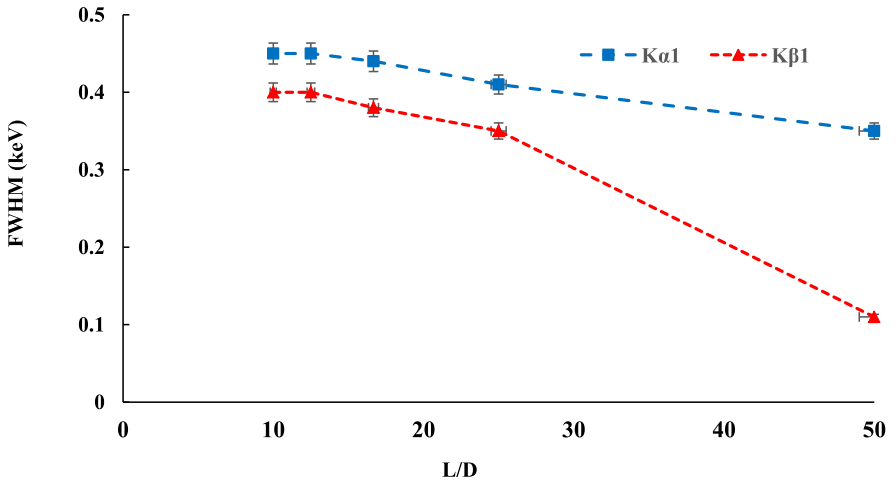

Fig. 9. FWHM values of Pd $K_{\alpha 1}$ and $K_{\beta 1}$ peaks as a function of collimator length-to-diameter ratio (L/D).

3.4. Fraction of dead time and uncertainty %

The uncertainties in relation to the Pd $K_{\alpha 1}$, Pd $K_{\beta 1}$ and Compton scattering peaks were almost linear and were connected to the L/D ratio of the collimator (Fig. 10). Increasing the L/D ratio of the collimator resulted in an increase in the uncertainties. This phenomenon was due to the decrease in the peak intensities with an increase in the L/D ratio of the collimator [18]. The fractional dead time decreased with an increase in the L/D ratio of the collimator, indicating the effect of a reduced intensity. This characteristically resulted in a nonlinear reduction of

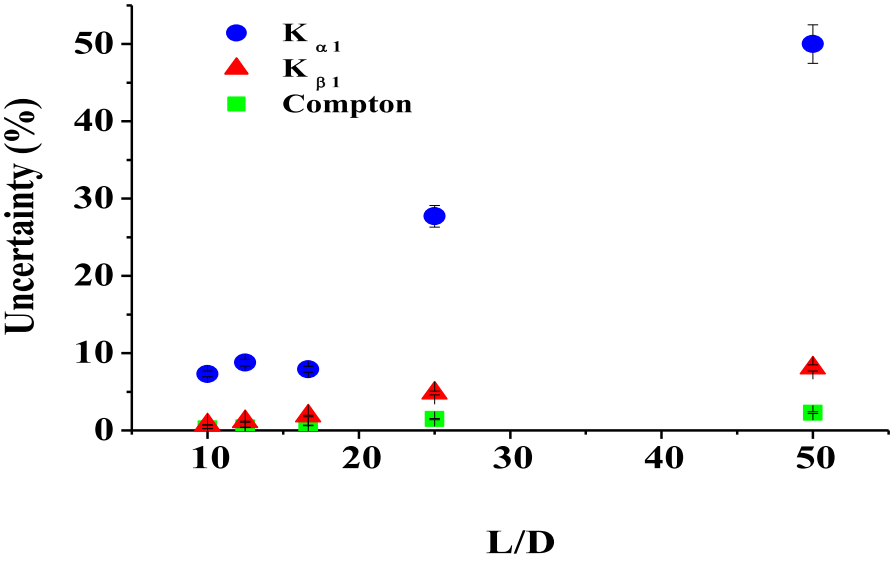

Fig. 10. Uncertainties in peaks of Pd $K_{\alpha 1}$, $K_{\beta 1}$, and Compton scattering as a function of the collimator length-to-diameter ratio (L/D).

https://doi.org/10.1016/j.heliyon.2018.e00724

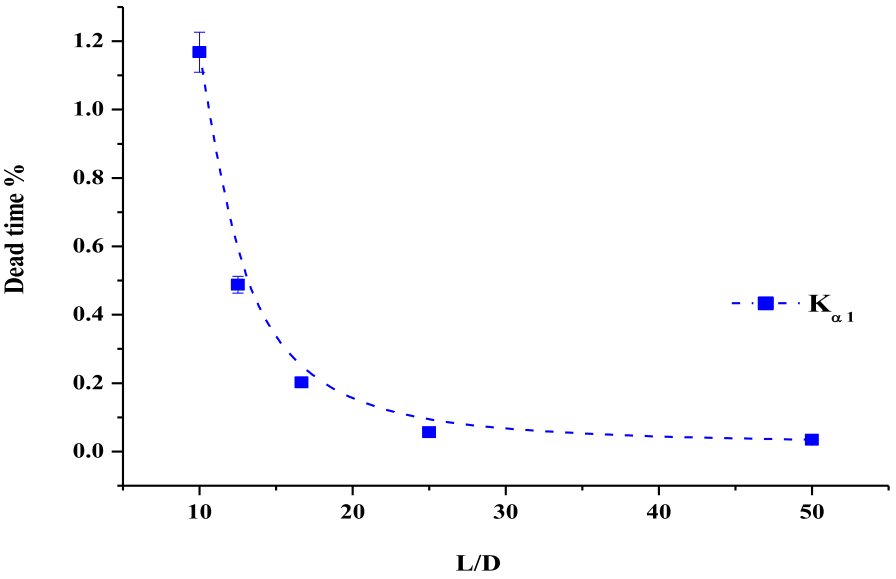

Fig. 11. Decline of dead time with collimator length-to-diameter ratio (L/D).

the measured intensity with the intensity irradiated to the detector. In addition, an increase in the diameter of the collimator (smaller L/D ratio) with the incident intensity resulted in a considerable percentage of this intensity being lost during the measurement, thereby increasing the dead time, but with a smaller uncertainty (Figs. 10 and 11).

4. Conclusion

The shielding of a detector with different collimator diameters was investigated to minimize the effect of Compton scattering. A collimator with a smaller diameter and larger L/D ratio was able to increase the peak resolution and reduce the Compton scattering and fractional dead time. However, the percentage of uncertainty was higher, indicating a reduction in the intensity of the XRF beam on the detector. Moreover, this resulted in the SCR being affected by the collimator diameter, in particular, and the shield of the detector, in general, where, for a fixed collimator length, the SCR was higher for a collimator with a diameter of 1 mm than for one with a diameter of 5 mm. This was because with an increase in the size of the collimator, the detector was more exposed to scattered radiation.

The use of a detector with a collimator had positive effects on the SNR compared to a detector without a collimator plug. In addition, the SNR increased with an increase in the collimator length-to-diameter ratio, thereby indicating that there was a minimum multiple scattering background when a narrow detector collimator was used. This process can be utilised to improve the effect of focusing the measurement on a sample that is to be irradiated by XRF.

https://doi.org/10.1016/j.heliyon.2018.e00724

Declarations

Author contribution statement

Mohammad W. Marashdeh: Conceived and designed the experiments; Performed the experiments; Analyzed and interpreted the data; Contributed reagents, materials, analysis tools or data; Wrote the paper.

Funding statement

This research did not receive any specific grant from funding agencies in the public, commercial, or not-for-profit sectors.

Competing interest statement

The author declares no conflict of interest.

Additional information

No additional information is available for this paper.

Acknowledgements

The author would like to thank members of Biomedical and Radiation Lab, School of Physics, University Sains Malaysia, USM, for technical assistance, which is greatly appreciated.

References

[1] G.F. Knoll, Radiation Detection and Measurement, John Wiley & Sons, 2010.

[2] A. Borella, T. Belgya, S. Kopecky, F. Gunsing, M. Moxon, M. Rejmund, P. Schillebeeckx, L. Szentmiklósi, Determination of the 209 Bi (n, γ) 210 Bi and 209 Bi (n, γ) 210m, g Bi reaction cross sections in a cold neutron beam, Nucl. Phys. A 850 (2011) 1−21.

[3] J. Scott, S. Lillicrap, 133Xe for the X-ray fluorescence assessment of gold in vivo, Phys. Med. Biol. 33 (1988) 859.

[4] A. Buffler, J. Tickner, Detecting contraband using neutrons: challenges and future directions, Radiat. Meas. 45 (2010) 1186−1192.

[5] J. Gräfe, F. McNeill, S. Byun, D. Chettle, M. Noseworthy, The feasibility of in vivo detection of gadolinium by prompt gamma neutron activation analysis following gadolinium-based contrast-enhanced MRI, Appl. Radiat. Isot. 69 (2011) 105−111.

https://doi.org/10.1016/j.heliyon.2018.e00724

[6] M. Singh, G. Singh, B. Sandhu, B. Singh, Effect of detector collimator and sample thickness on 0.662 MeV multiply Compton-scattered gamma rays, Appl. Radiat. Isot. 64 (2006) 373−378.

[7] L.J. Somervaille, D.R. Chettle, M.C. Scott, In vivo measurement of lead in bone using x-ray fluorescence, Phys. Med. Biol. 30 (1985) 929.

[8] J. O'meara, D. Chettle, F. McNeill, C. Webber, The feasibility of measuring bone uranium concentrations in vivo using source excited K x-ray fluorescence, Phys. Med. Biol. 42 (1997) 1109.

[9] R. Jonson, S. Mattsson, B. Unsgaard, A method for in vivo analysis of platinum after chemotherapy: with cisplatin, Phys. Med. Biol. 33 (1988) 847.

[10] T. Grönberg, K. Liden, S. Mattsson, T. Almen, S. Sjöberg, K. Golman, Non-invasive estimation of kidney function by x-ray fluorescence analysis. Method for in vivo measurements of iodine-containing contrast media in rabbits, Phys. Med. Biol. 26 (1981) 501.

[11] J.-O. Christoffersson, S. Mattsson, Polarised, X-rays in XRF-analysis for improved in vivo detectability of cadmium in man, Phys. Med. Biol. 28 (1983) 1135.

[12] P. Ali, C. Bennet, A. El-Sharkawi, D. Hancock, Optimisation of a polarised X-ray source for the in vivo measurement of platinum in head and neck tumours, Appl. Radiat. Isot. 49 (1998) 647−650.

[13] Y. Özdemir, B. Börekci, A. Levet, M. Kurudirek, Assessment of trace element concentration distribution in human placenta by wavelength dispersive X-ray fluorescence: effect of neonate weight and maternal age, Appl. Radiat. Isot. 67 (2009) 1790−1795.

[14] M.W. Marashdeh, S. Bauk, A.A. Tajuddin, R. Hashim, Measurement of mass attenuation coefficients of *Rhizophora spp.* binderless particleboards in the 16.59−25.26 keV photon energy range and their density profile using x-ray computed tomography, Appl. Radiat. Isot. 70 (2012) 656−662.

[15] R. Firestone, M. Krtička, Z. Revay, L. Szentmiklosi, T. Belgya, Thermal neutron capture cross sections of the potassium isotopes, Phys. Rev. C 87 (2013), 024605.

[16] N. Shengli, Z. Jun, H. Liuxing, EGS4 simulation of Compton Scattering for Nondestructive Testing, KEK proceedings, High Energy Accelerator Research Organization, 2000, 1999.

https://doi.org/10.1016/j.heliyon.2018.e00724

[17] ANSI/IEEE, IEEE Standard Test Procedures for Germanium Gamma-Ray Detectors, ANSI/IEEE Std. 325, Inst. of Elect. and Electronics Engineers, Inc., New York, USA, 1986.

[18] L. Luo, D.R. Chettle, H. Nie, F.E. McNeill, M. Popovic, The effect of filters and collimators on Compton scatter and Pb K-series peaks in XRF bone lead analysis, Nucl. Instrum. Methods Phys. Res. B 263 (2007) 258–261.

https://doi.org/10.1016/j.heliyon.2018.e00724